Proceedings of Ninth World Conference on Earthquake Engineering
August 2-9, 1988, Tokyo-Kyoto, JAPAN (Vol.II)

3-6-5

THE GROUND MOTION CHARACTERISTICS OF OFF FUKUSHIMA EARTHQUAKES AND THE SYNTHESIS FOR STRONG-MOTION BY FAULT SOURCE MODEL

Teruo SHIMIZU[1] Michiyasu TERADA[1]
Tsuyoshi SHIMADA[1] Makoto KAMIYAMA[2]

[1]Department of Nuclear Energy Development Division,
Kumagai Gumi Co.,Ltd., Shinjuku-ku, Tokyo, Japan
[2]Associate Professor, Department of Civil Engineering,
Tohoku Institute of Technology, Sendai, Japan

SUMMARY

To establish the local scaling law of seismic moment, a statistical analysis for velocity response spectra(h=0%) of seismic records of off Fukushima earthquakes is performed, a statistical scaling law is compared with the theoretical one by Sato and Hirasawa model. Based on the statistical analysis, a method for synthesizing strong motion from nonstationary spectra of small earthquake records is presented. The synthesized accelerograms and velocity response spectra(h=5%) using the proposed method show good agreement with recorded ones.

INTRODUCTION

As synthesizing strong motion from small earthquakes using faulting source model, it is hard to decide the number of sub-faults because seismic motion have two characteristics, frequency domain and time history. Irikura(Ref.1) decided the division numbers of fault plane of main shock and rise time from the seismic moment ratio and synthesized strong ground motions using observed small seismograms. Kamiyama(Ref.2) estimated the number of crack contained in fault by statistical analysis of fourier spectra and proposed the mothod for synthesizing strong ground motion by using fourier spectra.

We have been developing array seismic observation system KASSBM(Kumagai Gumi Array System for Strong Earthquake Motion) to clarify the characteristics of earthquakes and ground motion in coastal part of Miyagi and Fukushima Prefectures, Japan(Ref.3). In this study, using these observed records, the statistical and theoretical scaling law of off Fukashima earthquakes are shown and the synthesis method of strong ground motion from nonstationary spectra of small eathquakes taking account of the area of fault is proposed.

EARTHQUAKE SOURCE SPECTRAL RATIOS OF OFF FUKUSHIMA EARTHQUAKES

STATISTICAL ANALYSIS Fourier spectrum of earthquake motion, F(T) is expressed as follows

$$F(T) = I(T) \cdot G(T) \cdot R(T) \cdot S(T) \quad \cdots\cdots (1)$$

Where I(T):the frequency characteristics of instrument, G(T):frequency response function of local soil conditions, R(T):frequency response function of propagation media of waves, S(T): source spectrum, and T:period.

Considering the earthquakes occured in the same source area and observed at one observation site, it is reasonable to assume that each of I(T), G(T), R(T) in Eq.(1) is identical. Then, the fourier spectral ratio of two earthquakes

seems source spectral ratio, shown as follows.

$$F_1(T)/F_2(T) \fallingdotseq S_1(T)/S_2(T) \quad \cdots\cdots (2)$$

Then, calculating some source spectral ratios for a certain source area and carrying out statistical analysis, local statistical spectral ratios dependent on the variation of periods are obtained. The statistical model is proposed in the following expression introducing the power term of magnitude M to consider in detail the value of magnitude

$$\log_{10}(F_1(T)/F_2(T)) = a(T)(M_1^2 - M_2^2) + b(T)(M_1 - M_2) + c(T)(\log_{10}(\Delta_1 + 30) - \log_{10}(\Delta_2 + 30)) + d(T)(D_1 - D_2) + e(T) + \sum_{i=1}^{N-1} A_i(T) S_i \quad \cdots\cdots (3)$$

Where M_1, M_2: earthquake magnitude, Δ_1, Δ_2: epicentral distance, D_1, D_2: focal depth, S_i: dummy variable, a(T), b(T), c(T), d(T), e(T), $A_i(T)$: regression coefficient and, N: total number of observation sites.

The statistical model of Eq.(3) is applied for 182 accelerograms obtained at 8 observation sites from 13 earthquakes listed in Table 1. The observation sites and earthquake origins for these accelerograms are indicated in Fig.1. In the statistical analysis, S-2 site is selected as a base site. The regression coefficients a(T), b(T), c(T), d(T) and e(T) resulting from the statistical analysis of Eq.(3) are given in Fig.2. Fig.3 and Fig.4 show examples of spectral ratios obtained from observed records and from results of the statistical analysis, respectively. The statistical spectral ratios are smoother than recorded ones, and both spectral ratios resemble each other.

THEORETICAL ANALYSIS Following Sato and Hirasawa(Ref.4), the acceleration fourier spectrum F(T) in a far-field point is given as

$$F(T) = [M_0/(4\pi\rho r_0 Vs^3)] \cdot |R(\theta, \phi)| \cdot |B(T)| \quad \cdots\cdots (4)$$

Where M_0: seismic moment, r_0: radius of fault, Vs: shear wave velocity, $R(\theta, \phi)$: radiation pattern, and B(T): normalized source spectrum.

Considering the earthquakes occured in the same source area, each of Vs and $R(\theta, \phi)$ can be assumed to be identical. Then theoretical source spectral ratio is expressed as follows.

$$F_1(T)/F_2(T) = (M_{01} \cdot r_{02}/M_{02} \cdot r_{01}) \cdot |B_1(T)|/|B_2(T)| \quad \cdots\cdots (5)$$

Fig.5 shows examples of the theoretical spectral ratios calculated on conditions assumed as Table 2 (Ref.5). Comparing the theoretial spectral ratios with the statistical ones, a small difference can be found the longer period range (2～5sec) but total tendency of both spectral ratios coincides closely.

A METHOD FOR SYNTHESIZING EARTHQUAKE MOTIONS USING NONSTATIONARY SPECTRA

Nonstationary spectrum of earthquake motion resolved into time and period domains is obtained by multipling earthquake motion f(t) by a certain window function $h_e(t-\tau)$ and integrating it in time domain.

$$F(w, t) = \left| \int f(t) \cdot h_e(t-\tau) e^{-iw} d\tau \right| \quad \cdots\cdots (6)$$

Thus, strong motion systhesis can be performed by superposing nonstationary spectra of small earthquakes over time and period domains taking the fault model and source spectral ratio into consideration.

SYNTHESIZING METHOD 1) The following exponential function which has four parameters as shown in Fig.6 is adopted for the model of F(w, t)

$$M(w_n, t) = \begin{cases} A(w_n) \exp[(t - T(w_n))/B(w_n)] & , t \leqq T(w_n) \\ A(w_n) \exp[(T(w_n) - t)/L(w_n)] & , t > T(w_n) \end{cases} \quad \cdots\cdots (7)$$

Where $A(w_n)$: the maximum amplitude, $T(w_n)$: the time when the maximum exists, $B(w_n)$, $L(w_n)$: constants for model function by exponential function before

and after the peak, respectively.

2) Statistical analysis for four parameters is excuted by using following regression model

$$\log_{10}P_j(w)=a_j(w)M^2+b_j(w)M+c_j(w)\log_{10}(\Delta+30)+d_j(w)D+e_j(w)+\sum_{i=1}^{N-1}A_{ij}(w)S_{ij} \quad \cdots\cdots (8)$$

Where $P_j(W)$ $(j=1,\cdots,4)$ is $A(w_n)$, $T(w_n)$, $B(w_n)$, $L(w_n)$, respectively.

3) Estimate the nonstationary spectrum of element earthquake $Me(w,t)$ from Eq. (7) and Eq. (8) giving appropriate values of M, Δ, D, and $S_i(i=1,\cdots,7)$ based on the results of statistical analysis.

4) Using the empirical relationships indicated in Table 2, calculate the source area S, seismic moment M_0. The number of superposition N_f decides seismic moment ratio between large earthquake and element one. The source plane is assumed as Fig. 7.

5) Distribute the modeled nonststationary spectra of element earthquake $Me(W_n,t)$ based on the results of statistical analysis on the fault plane and superpose them considering the time lag for expanding element faults.

$$Mm(w,t)=\sum_{i=1}^{Nf}Me(w,\ t-t_{di}) \quad \cdots\cdots (9)$$

$$t_{di}=d_i/Vr+(r_i-r_0)/Vc$$

Where $Mm(w,t)$, $Me(w,t)$: the modeled nonstationary spectra of large earthquake and element one, respectively, N_f: number of element earthquake, t_{di}: time lag, Vr: rupture velocity, Vc: propagation velocity of eathquake wave and d_i, r_i, r_0 are defined in Fig. 7.

6) After superposing, modify the amplitude of $Mm(w,t)$ taking account of source spectral ratios as follows

$$Fm(w,t)=Ae(w)\cdot Rme(w)\cdot Mm(w,t)/Am(w) \quad \cdots\cdots (10)$$

Where $Fm(w,t)$: nonstationary specrtum of large earthquake, $Am(w)$, $Ae(w)$: the maximum amplitude of $Mm(w,t)$ and $Me(w,t)$, respectively, $Rme(w)$: source spectral ratio between large earthquake and element one.

7) Replacing Eq. (10) into Eq. (6) and transforming Eq. (6) inversely, the strong earthquake motion of large earthquake is obtained.

THE RESULTS OF ANALYSIS Multiple correlation coefficients of four parameters from statistical analysis are shown in Fig. 8. The coefficient of A(w) has a higher value over the whole period range. On the other hand, the coefficients of T(w), B(w), L(w), related to time domain are lower then that of A(w). The difference is caused by the characteristic of model function of nonstationary spectrum and uncertainty of these parameters depending on time.

The synthesized motions at S-2 and S-5 on conditions listed in Table 3 are shown in Fig. 9 and Fig. 10, respectively. Fig. 9(a) and Fig. 10(a) show the synthesized motions by using statistical spectral ratios and Fig. 9(b) and Fig. 10 (b) are obtained by using theoretical ones of Sato and Hirasawa model. The observed motions are shown in Fig. 9(C) and Fig10. (C). Comparing both synthesized motions with observed ones, though the maximum accelerations of synthesized motions are a little larger than observed ones, the principal part of motions and velocity response spectra (h=5%) of synthesized motions have consistent features with the observed ones. Paying attention to S-5 set on a soft ground, the proposed synthesizing method cannot completely explain the longer period components (2～5sec) appearing in the latter part of observed accelerograms.

Finally, Fig. 11 shows the synthesized strong motions of M=8 earthquake which have never occured in the region from M=6.5 earthquakes using source spectral ratios of Sato and Hirasawa model.

CONCLUSIONS

The principal conclusions drawn from this study are summarized as follows.

1) The source spectral ratios obtained from statistical analysis of velocity response spectra(h=0%) of observed accelerograms show good agreement with the theoretical ones. Especially, if the difference in magnitude between large and small earthquakes is about 1, the spectral ratios between them closely resemble the theoretical spectral ratios.

2) The method of synthesizing ground motion proposed in this study, using nonstationary spectra and source spectral ratios is useful to simulate recorded ground motions.

3) The proposed method by using the theoretical spectral ratios makes it possible to estimate a strong motion which has never occured in a certain region.

4) The time duration of the synthesized motions, especially in the longer period range (2～5sec) is influenced by modeling of nonstationary spectra of earthquake motions.

REFERENCES

1. Irikura, K., "Semi-Empirical Estimation of Strong Ground Motions During Large Earthquakes," Bull. Disast. Prev. Res. Inst., 33, 63-103, (1983).
2. Kamiyama, M., "Earthquake Source Characteristics Inferred from the Statistically Analyzed Spectra of Strong Motions with Aid of Dynamic Model of Faulting," Proc. of JSCE, 4, 391-400, (1987).
3. Abe, K., Shimizu, T., Kasuda, K., and Yanagisawa, E., "The Development of the Dense Instrument Array System 'KASSEM' and the Analysis of Observed Earthquake Waves," Proc. 9WCEE, (in print), (1988).
4. Sato, T. and Hirasawa, T., "Body Wave Spectra from the Propagation Shear Cracks," J. Phys. Earth., 21, 415-431, (1973).
5. Sato, R., "Theoretical Basis on Relationships between Focal Parameters and Earthquake Magnitude," J. Phys. Earth., 27, 353-372, (1979).

Table 1 Observed Earthquakes

No	Date	Magnitude	Comp.	Maximum Accelaration							
				S-1	S-2	S-3	S-4	S-5	S-6	S-7	S-8
1	1985. 5.11	5.3	NS EW	24.8 23.8	4.0 6.7	—	8.0 7.3	—	7.2 7.0	22.2 20.0	106.1 94.2
2	7.29	4.7	NS EW	18.3 15.4	4.9 4.4	6.1 6.2	6.4 7.0	12.6 10.5	—	23.3 18.6	51.8 70.2
3	8.12	6.4	NS EW	16.4 18.4	20.0 27.2	61.7 52.0	21.8 24.0	55.0 84.6	—	47.0 39.0	70.2 85.3
4	1986. 5. 5	4.9	NS EW	30.3 22.2	3.6 4.6	7.1 7.2	7.9 8.7	13.6 11.6	4.8 5.3	17.7 19.2	21.4 24.4
5	1987. 2. 6	6.4	NS EW	13.8 17.0	14.4 19.5	25.8 17.1	12.3 14.9	25.3 28.2	23.8 20.4	20.7 25.1	82.2 97.4
6	2. 6	6.7	NS EW	31.5 29.1	25.1 41.7	47.1 43.4	22.0 30.9	67.9 55.4	55.6 52.0	70.6 40.3	208.1 183.9
7	2.28	5.6	NS EW	—	24.9 17.7	15.8 15.8	—	31.4 22.4	15.4 12.5	21.7 16.7	14.5 14.1
8	3. 1	4.7	NS EW	—	9.2 4.5	7.0 6.7	—	15.0 12.9	8.3 5.9	13.6 13.3	14.1 17.2
9	3.10	5.6	NS EW	—	4.2 5.0	6.6 5.2	—	9.8 9.8	9.6 6.1	11.7 8.6	20.5 21.6
10	4. 7	6.6	NS EW	—	77.9 102.9	61.0 65.2	—	85.7 125.0	82.3 100.4	231.2 218.3	235.7 275.8
11	4.17	6.1	NS EW	31.1 24.7	6.5 10.8	12.5 10.7	13.5 11.6	20.9 21.7	12.1 12.9	35.0 23.6	64.1 87.9
12	4.20	5.1	NS EW	—	5.8 12.2	12.3 8.0	10.4 15.8	19.1 18.3	17.4 27.6	24.8 23.1	35.5 28.1
13	4.23	6.5	NS EW	35.8 39.0	30.0 42.5	64.3 41.1	31.5 41.7	59.5 55.4	89.9 52.6	82.8 66.1	277.0 275.0

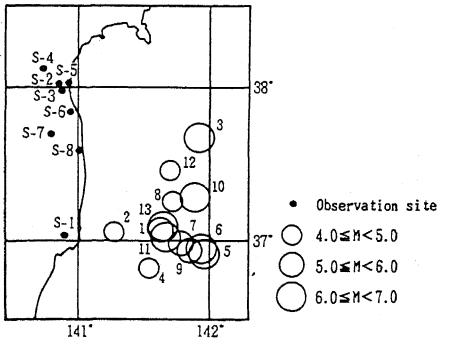

Fig. 1 Location of Observation Sites and Distribution of Epicenter

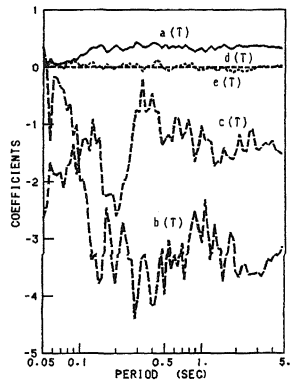

Fig. 2 Regression Coefficients of a(T), b(T), c(T), d(T), e(T) in Eq. (3)

Table 2 Fault Parameters to Calculate Theoretical Spectral Ratios

Share Wave Velocity	$Vs = 4.0 km/sec$
Rapture Velocity	$Vr = 0.72Vs$
Seismic Moment	$M_o = 10^{1.5M+16}$
Fault Area	$S = 10^{M-4.07}$
Fault Radius	$r_o = (S/\pi)^{0.5}$

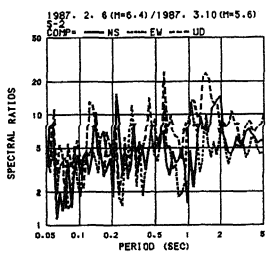

(a) 1987. 2. 6(M=6.4)/1987. 3.10(M=5.6)

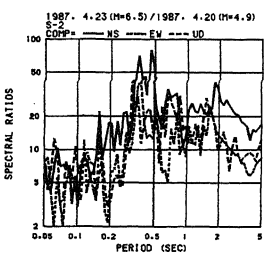

(b) 1987. 4.23(M=6.5)/1987. 4.20(M=4.9)

Fig. 3 Examples of Spectral Ratios of Observed Records at S-2

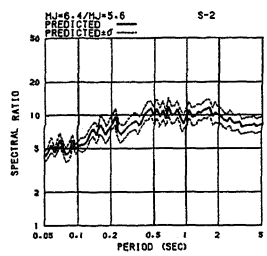

(a) M=6.4/M=5.6

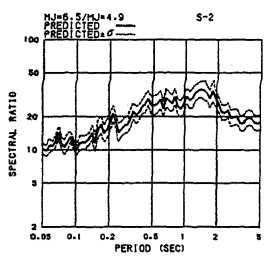

(b) M=6.5/M=4.9

Fig. 4 Examples of Statistical Spectral Ratios at S-2

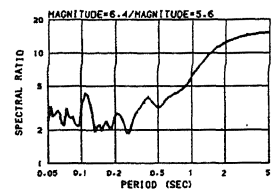

(a) M=6.4/M=5.6

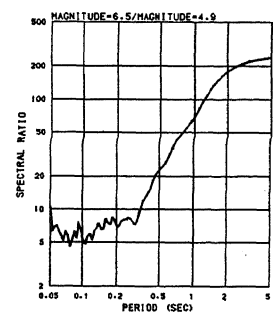

(b) M=6.5/M=4.9

Fig. 5 Examples of Theoretical Spectral Ratios by Sato and Hirasawa Model

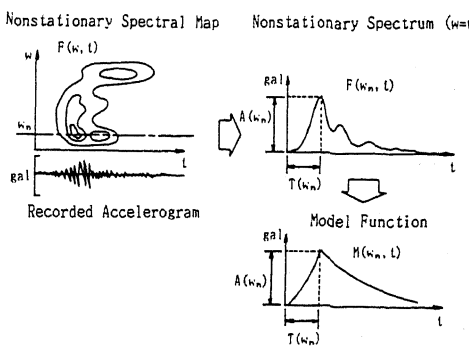

Fig. 6 Modeling of Nonstationary Spectrum

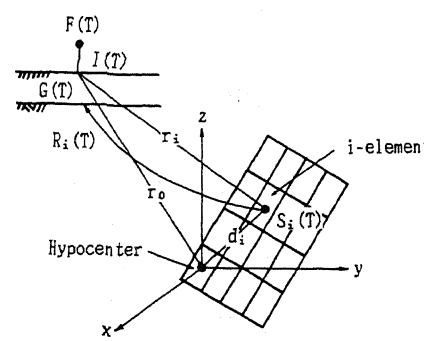

Fig. 7 Fault Model

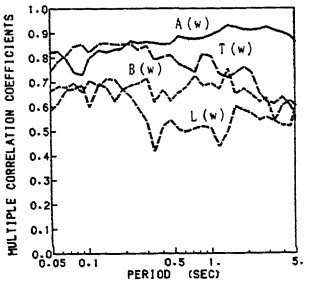

Fig. 8 Multiple Correlation Coefficients of A(w), T(w), B(w), L(w) in Eq. (8)

Table 3 Fault Parameters to Synthesize Earthquake Motions

Magnitude of Main Shock	6.4
Magnitude of Event Shock	5.6
Fault Length	24km
Fault Width	12km
Center of Fault	N36° 56.2′ E141° 56.1′
Share Wave Velocity	4.0km/sec
Rapture Velocity	2.9km/sec
Strike Direction	N10° E
Dip Angle	60° W
Division of Fault	4 × 4

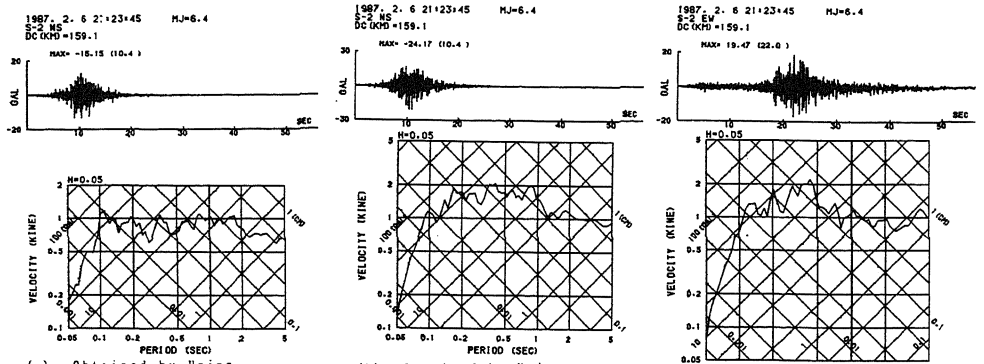

(a) Obtained by Using Statistical Spectral Ratio (b) Obtained by Using Theoretical Spectral Ratio (c) Observed Accelerogram

Fig. 9 Comparison of the Synthesized Accelerograms and Velocity Response Spectra (h=5%) with Observed Ones at S-2

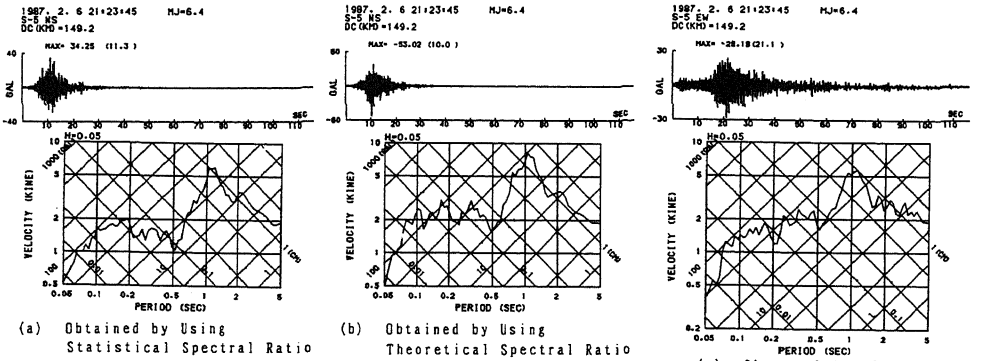

(a) Obtained by Using Statistical Spectral Ratio (b) Obtained by Using Theoretical Spectral Ratio (c) Observed Accelerogram

Fig. 10 Comparison of the Synthesized Accelerograms and Velocity Response Spectra (h=5%) with Observed Ones at S-5

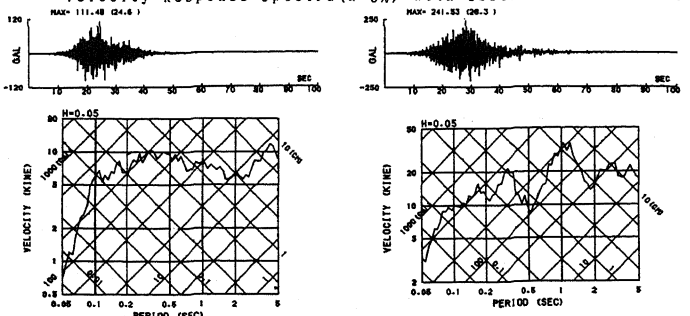

(a) S-2 (b) S-5

Fig. 11 Synthesized Accelerograms and Velocity Response Spectra (h=5%) of M=8.0 Earthquake from M=6.5 Element Earthquakes